CHAPTER 4
SUPERPARAMAGNETIC FLEXIBLE SUBSTRATES BASED ON SUBMICRON ELECTROSPUN ESTANE® FIBERS CONTAINING MnZnFe-Ni NANOPARTICLES

4.1 Chapter Summary

Flexible field responsive superparamagnetic substrates were prepared by electrospinning a solution of elastomeric polyurethane containing ferrite nanoparticles (ca. 14 nm) of Mn-Zn-Ni. The flexible mats were characterized in terms of fiber morphology and magnetic properties. Field Emission Scanning Electron Microscopy (FESEM) indicated that the diameter of these composite fibers was ca. 300-500 nm. Furthermore, the back-scattered electron FESEM images indicated agglomeration of the nanoparticles at higher wt% (ca 17-26 wt%) loading on the electrospun fibers. The induced specific magnetic saturation and the relative permeability were found to increase with increasing wt% loading of the ferrite nanoparticles on the submicron electrospun fibers. A specific magnetic saturation of 1.7 – 6.3 emu/g at ambient conditions indicated superparamagnetic behavior of these composite electrospun substrates.

4.2 Introduction

The ability to produce one-dimensional magnetic nanostructures in the form of fibers is very attractive as these are expected to exhibit interesting magnetic-field dependent properties. These materials could be used as active components for ultra-high density storage applications,[1] as well as in the fabrication of sensors.[2,3] Other potential applications include magnetic filters[4] and future generations of electronic, magnetic and/or photonic devices ranging from information storage, magnetic imaging to static and low frequency magnetic shielding and magnetic induction.[5-8] One of the commonly used methods to produce one-dimensional nanostructures is based on the electrodeposition of magnetic materials on porous membranes.[9] This technique has been applied to fabricate metallic nanowires that have displayed anisotropic magnetic properties. However, such a technique is limited when applied to oxide-based magnetic materials (e.g. ferrite) due to the technical difficulties involved in the formation of oxides through the electrochemical deposition process.

Ferrites are widely used in many industrial applications due to their spontaneous magnetization. Therefore, the development of new and cost-effective techniques for fabricating nanostructures based on ferrites is of great commercial and scientific interest. In particular, soft ferrites[10-12] of Mn-Zn, Ni-Zn and Mg-Mn are well known for their high magnetic permeability.[13] Current research efforts[14] have been focused on synthesizing nanometer sized (5-20 nm) ferrite particles to minimize energy losses associated with bulk systems. Below a diameter of ca. 100 nm, particles of mixed[15] ferromagnetic materials (such as ferrites of Mn-Zn-Ni), do not exhibit the cooperative phenomenon of ferromagnetism found in the bulk as the thermal vibrations are sufficient to reorient the magnetization direction of the magnetic domains.[16] As a result, such nanoparticles display superparamagnetic behavior. When incorporated in submicron (200-500 nm) polymeric fibers, flexible superparamagnetic materials can be produced in a relatively convenient (in comparison to the electrochemical deposition process) and cost-effective fashion. In the present investigation, we report the processing of such substrates where nanoparticles of a mixed ferrite of Mn-Zn-Ni were incorporated in submicron (200-500 nm) fibers of an elastomeric polymer (a polyester based segmented polyurethane) via electrospinning.

Electrospinning is a unique process to produce submicron polymeric fibers in the average diameter range of 100 nm-5 μm[17-20]. Fibers produced this way are at least one or two orders of magnitude smaller in diameter than those produced by conventional fiber production methods like melt or solution spinning.[21] In a typical electrospinning process (Figure 4.1), described extensively in the literature,[22-26] a jet is ejected from the surface of a charged polymer solution when the applied electric field strength (and consequently the electrostatic repulsion on the surface of the fluid) overcomes the surface tension. The ejected jet travels rapidly to the collector target located at some distance from the charged polymer solution under the influence of the electric field and becomes collected in the form of a solid polymer filament as the jet dries. During its flight to the target, the jet undergoes a series of electrically driven bending instabilities[27-31] that gives rise to a series of looping and spiraling motions. In order to minimize the instability caused by the repulsive electrostatic charges, the jet elongates to undergo large amounts of plastic stretching that consequently leads to a significant reduction in its diameter. These

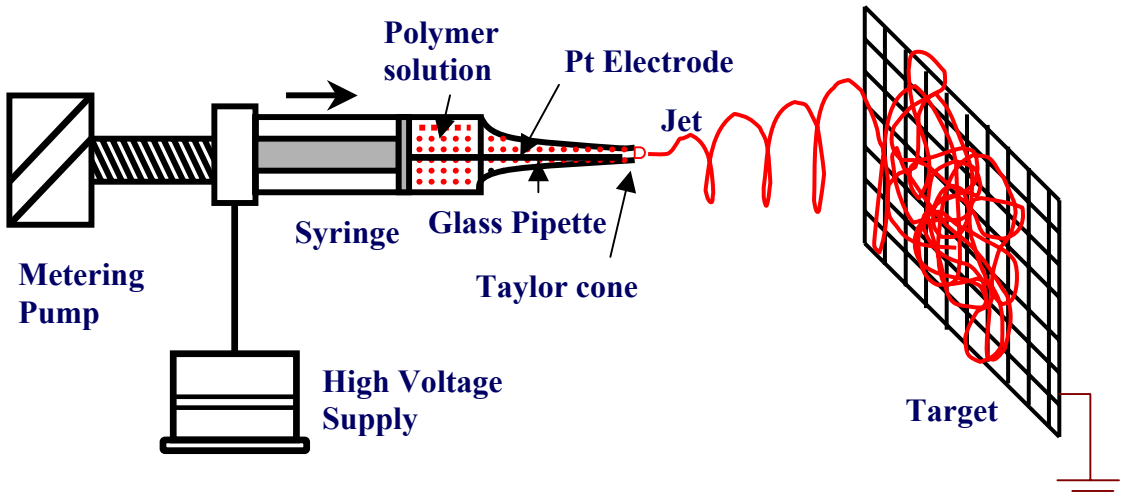

Figure 4.1 Schematic of the electrospinning apparatus utilized to electrospin Estane®-MnZnFe-Ni solutions.

extremely small diameter electrospun fibers possess a high aspect ratio that promotes a larger specific surface. As a result, they have potential applications ranging from optical[32,33] and chemo-sensor materials,[34] nanocomposite materials,[35] nanofibers with specific surface chemistry[36] to tissue scaffolds, wound dressings, drug delivery systems,[25,26,37-44] filtration and protective clothing.[45]

Very recently, magnetic ceramic nanofibers of nickel ferrite were produced by post-electrospinning calcination of PVP/metal alkoxide precursors. The substrates displayed *significant* magnetic hysteresis that could significantly hamper its response in certain high frequency (MHz) magnetic applications.[13,14] In comparison, electrospinning of a solution containing *well-dispersed* superparamagnetic *nanoparticles* of soft and mixed ferrites leads to the formation of substrates that have very small energy losses. An interesting application of flexible superparamagnetic substrates could be based on their response to high frequency (MHz) magnetic fields. This becomes relevant where attenuation of the radio signal intensity is required to facilitate better communication in the RF. Such an application is particularly important for the armed forces, where in uneven terrain, the signal intensity received by the radio antenna embedded in the textile

uniform of a soldier, becomes very poor, thereby leading to poor radio communication.[46] As a result, the need to produce *flexible* superparamagnetic materials that could potentially serve as a radio antenna reflectors becomes very relevant. In the present investigation, we report our attempts to process such 'smart' (*flexible and superparamagnetic)* materials by electrospinning a polymer solution of an elastomeric polymer (a polyester based segmented polyurethane) containing nanoparticles of a mixed ferrite of Mn-Zn-Ni. A similar approach was utilized by Wang et al[16], where superparamagnetic composite polymer/magnetite nanofibers were produced. These materials were suggested to be utilized for reinforcement and nanocomposite applications, however, the targeted applications of the substrates discussed in the present investigation are very different. Here, superparamagnetism, *flexibility* and *high frequency response* are critical.

4.3 Experimental

4.3.1 Materials

Estane® 5750, a polyester based segmented polyurethane supplied by Noveon Inc., in the form of pellets was utilized for this study. Molecular weight data for Estane® 5750 could not be obtained, as the information was deemed proprietary, but the chemical structure[47] is depicted in Figure 4.2. N,N-dimethylacetamide (DMAc) was procured from Sigma Aldrich and was used without any further purification. Estane® was dissolved in DMAc at a concentration of 20 wt% by constant stirring for 4h at 65 ^{o}C. Superparamagnetic ferrite nanoparticles (ca. 14 nm) based on MnZnFe-Ni, that were dispersed in ethanol at a concentration of 5 and 10 wt% were procured from NanoSonic Inc. A transmission electron micrograph (TEM) of the nanoparticles is shown in Figure 4.3. The dark spots that represent the nanoparticles indicate the size to be ca. 14 nm. The solution of ferrite nanoparticles was mixed with Estane® solution at different ratios to make four solution-blends (Table 4.1). These were subsequently utilized for electrospinning to make composite electrospun substrates that had varying amounts of loading of the nanoparticles on the Estane® fibers. It should be noted that ethanol and DMAc are compatible solvents; as a result, the two solutions were easily mixed to obtain the four-component solutions. However, due to an extremely large ratio of the densities of the polymer and the magnetic nanoparticles (ca. 1 to 7), the heavier nanoparticles in

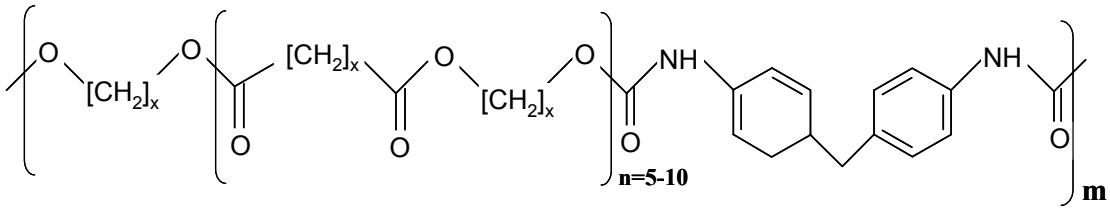

Figure 4.2 Chemical Structure[47] of Estane®.

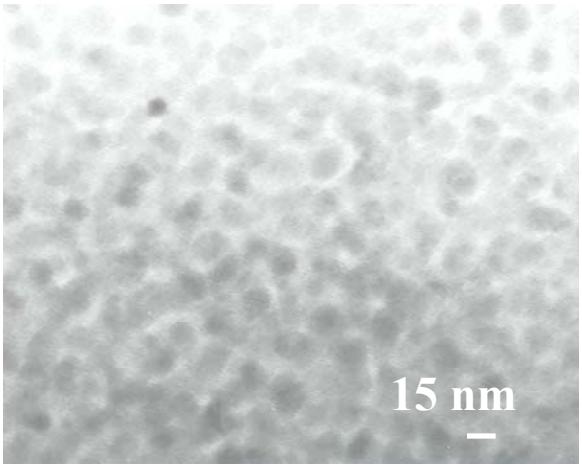

Figure 4.3 TEM of MnZnFe-Ni nanoparticles.

Table 4.1 Characterization of solutions, electrospinning conditions and wt% loading of ferrite nanoparticles on solid, dry composite fibers.

Total solids concentration in solution, wt%	**Zero shear rate viscosity Pa.s**	**Conductivity μS**	**Electrospinning conditions (potential drop, flow rate and target distance)**	**Loading of MnZnFe-Ni on solid, dry Estane® - MnZnFe-Ni fibers wt%**
17.0	3.0 ± 0.02	54	17 kV, 3 ml/h, 15cm	6
17.7	3.6 ± 0.07	63	18 kV, 3 ml/h, 15 cm	11
16.7	1.9 ± 0.05	97	20 kV, 3 ml/h, 14 cm	18
15.6	1.1 ± 0.18	203	17 kV, 3 ml/h, 14 cm	26

the solution were observed to settle down due to gravity within a period of 48 h, if left undisturbed. Therefore, these solutions were stirred vigorously before electrospinning to achieve sufficient dispersion of the nanoparticles.

4.3.2 Electrospinning and Characterization

Prior to electrospinning, the viscosities of these solutions were measured with an AR-1000 Rheometer, TA Instruments Inc. The measurement was performed in the continuous ramp mode at room temperature (25 ^{o}C) using cone and plate geometry. The sample solution was placed between the fixed Peltier plate and a rotating cone (diameter: 4 cm, vertex angle: 2^{o}) attached to the driving motor spindle. The changes in viscosity and shear stress with change in shear rate were measured. A computer interfaced to the equipment recorded the resulting shear stress vs. shear rate data. All the solutions investigated in this study displayed shear thinning behavior at high shear rates (viscosity-shear rate curves not shown). The initial slope of the shear stress-shear rate behavior where Newtonian behavior was observed gave the zero shear rate viscosity, η_o. The zero shear viscosities of the four solutions investigated in this study are reported in Table 4.1. An Oakton® conductivity tester, model TDStestr 20 was utilized to measure the conductivity of the polymer solutions. Prior to its use, the conductivity tester was calibrated by standard solutions procured from VWR Scientific®. The conductivity of the four solutions investigated in the present study is also reported in Table 4.1.

Electrospinning of these solutions was done on an apparatus depicted in Figure 4.1. The syringe containing the polymer solution was connected to a Teflon needle (0.7 mm internal diameter). A platinum electrode, placed in the syringe that was immersed in the polymer solution, was connected to a high voltage DC supply at a positive polarity. A syringe-pump connected to the wide-end of the syringe controlled the flow rate emanating out of the Teflon needle tip. Electrospun materials were collected on a grounded steel wire mesh that served as the target kept at ca. 15 cm from the Teflon tip. The diameter of the steel wire mesh was ca. 0.5 mm with a mesh count of 20x20 (20 steel wires per 1" each in the horizontal and vertical axes). All solutions were electrospun at 25 ^{o}C, 17-20 kV, 3ml/h with a 14-15 cm separation distance between the target and Teflon tip (Table 4.1). The fibrous mats were subsequently dried in a vacuum oven for 8h at 60 ^{o}C to minimize any residual solvent.

A Leo® 1550 Field Emission Scanning Electron Microscope (FESEM) was utilized to visualize the morphology of the composite electrospun fibers. All the images were taken in the back-scattered mode, as the back-scattered detector is more sensitive to the electron density differences arising due to the presence of different chemical species, viz. ferrite nanoparticles and the polymer. A Cressington® 208HR sputter-coater was utilized to sputter-coat the electrospun fiber samples with a 10 nm Pt/Au layer to minimize the electron charging effects.

Magnetic properties of composite electrospun substrates were characterized at ambient by utilizing a LakeShore 7300 Vibrating Sample Magnetometer (VSM). A sample of ca. 0.05 g was placed between two coils of an electromagnet that produced a uniform magnetic field gradient. The applied magnetic field induced the magnetic domains to directionally align along the magnetic field. During this induced alignment of the domains, the motion of the ferrite particles produced an electrical signal in a set of stationary pick-up coils that was proportional to the magnetic moment, vibration amplitude, and vibration frequency of the ferrite particles. The magnetic field was ramped from 8000 Gauss to -8000 Gauss and back to 8000 Gauss over a period of 30 minutes. The magnetic moment of each magnetic sample was measured with a sensitivity of 0.1 emu/g. The specific magnetic saturation values of the composite electrospun substrates were calculated for each electrospun substrate by dividing the saturation magnetization with its mass. Table 4.2 lists the specific magnetic saturation in addition to absolute permeability and relative permeability of composite electrospun substrates.

4.4 Results and Discussion

As discussed above, four different solutions were made by mixing the Estane® solution (at 20wt% in DMAc) with the MnZnFe-Ni nanoparticles solutions (at 5 and 10 wt% in ethanol). The total solids concentration of these solutions along with the zero shear viscosity and conductivity of the four solutions are reported in Table 4.2. It can be seen that the zero shear viscosity follows the same trend as the total concentration solids in ethanol and DMAc when plotted as a function of the wt% loading of nanoparticles on Estane® fibers (Figure 4.4a&b). Furthermore, the conductivity of the solutions was found to increase with an increase in the loading of the nanoparticles, as was expected (Figure 4.4c). Electrospinning of these four solutions resulted in four flexile substrates that had

Table 4.2 Magnetic saturation, absolute and relative permeability of Estane-MnZnFe-Ni composite submicron fibers.

Fiber Samples	Magnetic Saturation (emu/g)	Absolute Permeability* (μ) (H/m)	Relative Permeability (μ_r)
Estane® w/ ***6%*** MnZnFe-Ni	1.71	2.26×10^{-6}	1.80
Estane® w/ ***11%*** MnZnFe-Ni	2.99	3.84×10^{-6}	3.06
Estane® w/ ***18%*** MnZnFe-Ni	4.38	5.88×10^{-6}	4.68
Estane® w/ ***26%*** MnZnFe-Ni	6.33	8.23×10^{-6}	6.55
Pure MnZnFe-Ni	25.47	3.45×10^{-5}	27.46

* *Vacuum permeability* 1.257×10^{-6} *H/m*

different wt% loading (6, 11, 17 and 26 wt%) of MnZnFe-Ni nanoparticles on the Estane® fibers. Interestingly, all the four flexible composite substrates did not display any electrical conductivity. This might be useful for certain applications, where magnetic behavior may be desired but without any electrical conductivity.

The backscattered FESEM images of the four substrates, as shown in Figure 4.5, indicated the electrospun fiber diameter to be ca. 300-500 nm. Furthermore, the high electron density ferrite nanoparticles appeared as white spots in these images, which became more apparent at higher wt% loading of the nanoparticles. The increased fiber roughness and larger white spots at higher wt % loading indicated some agglomeration of the nanoparticles in the fibers. However, the agglomeration of the nanoparticles did not affect the overall magnetization behavior of these substrates. This was apparent in Figure 4.6 where magnetization curves recorded at ambient conditions indicated superparamagnetic behavior of these substrates. The magnitude and direction of the induced specific magnetization varied accordingly with the magnitude and direction of the applied magnetic field. To better observe any magnetic hysteresis, the region close to the origin is enlarged in the inset in Figure 4.6. It can be clearly seen that these flexible substrates have very little magnetic hysteresis with a small residual magnetization at zero

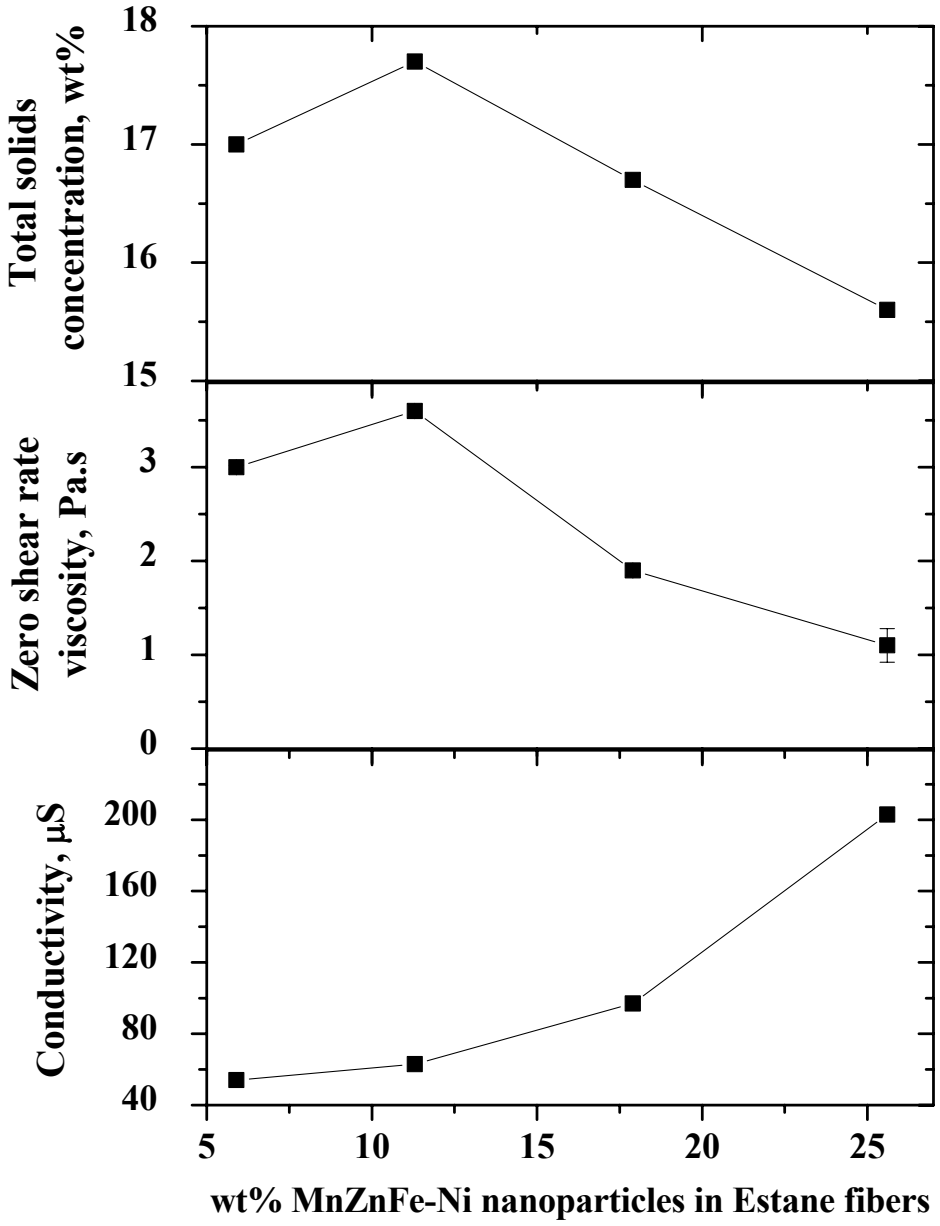

Figure 4.4 Characterization of solutions: a) Total solids concentration, b) Zero shear rate viscosity and c) conductivity as a function of wt% of ferrite nanoparticles.

magnetic field. The observed values of the specific magnetic saturation (1-6 emu/g) of the electrospun substrates were very low in comparison to that of bulk materials (ca. 150 emu/g for Fe-Co[48]), however it is important to note that the bulk materials have much larger hysteresis due to the large scale cooperative association of the magnetic domains.

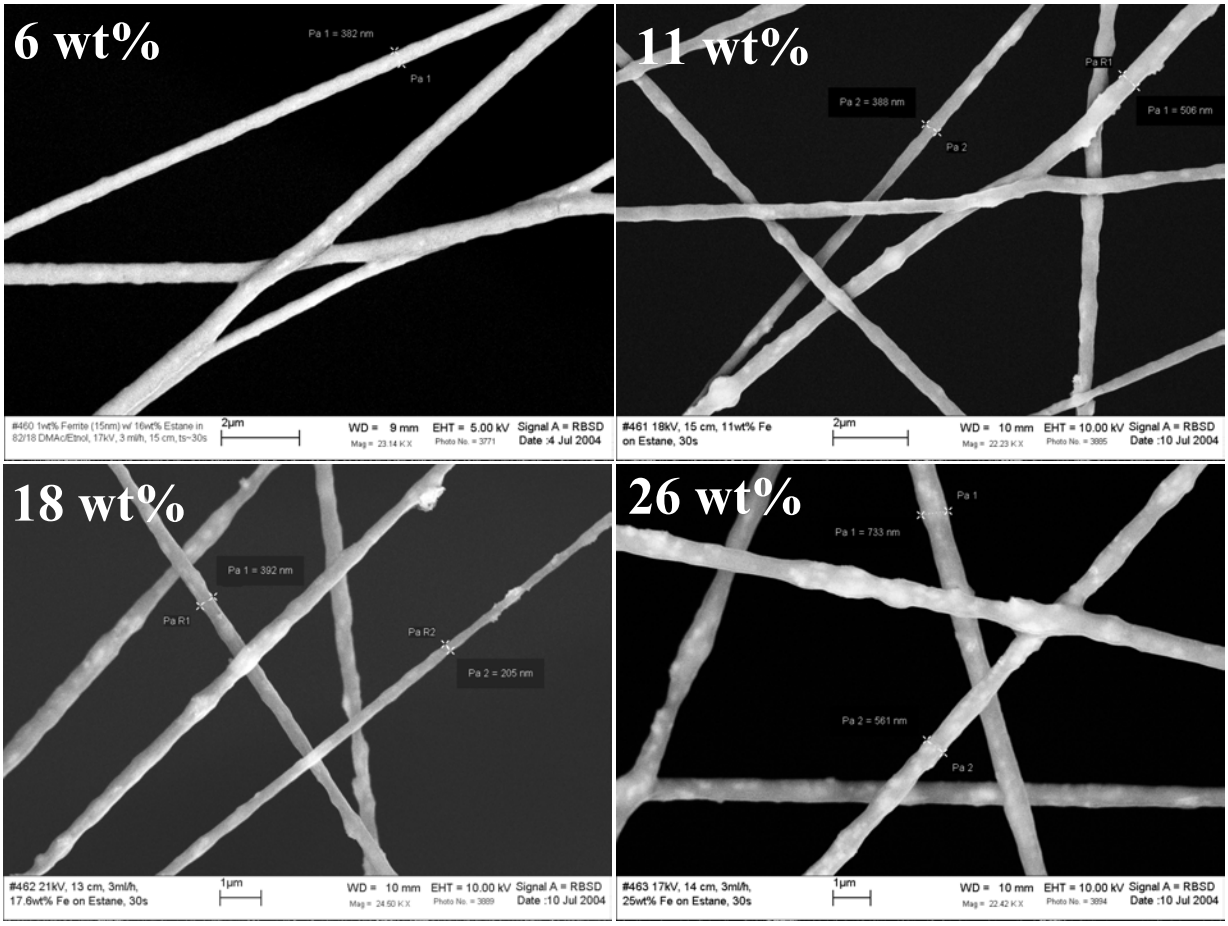

Figure 4.5 Backscattered SEM images of electrospun Estane®-MnZnFe-Ni composite fibers at different concentrations of MnZnFe-Ni nanoparticles. Note the distinctive change in fiber surface contrast at higher loading of nanoparticles. The lighter (high electron density) regions are rich in MnZnFe-Ni nanoparticles.

It is believed that the very little hysteresis in the electrospun substrates investigated in this study, might be critical in governing the magnetic behavior in a high frequency application. As expected, the specific saturation magnetization increased with increasing wt% loading of the nanoparticles as shown in Figure 4.7a. A linear correlation between the saturation magnetization and the wt% loading of nanoparticles with a very high regression (R^2=0.999) was observed. Likewise, the relative permeability, which is the ease with which a magnetic flux can be induced in a material, was also plotted with the

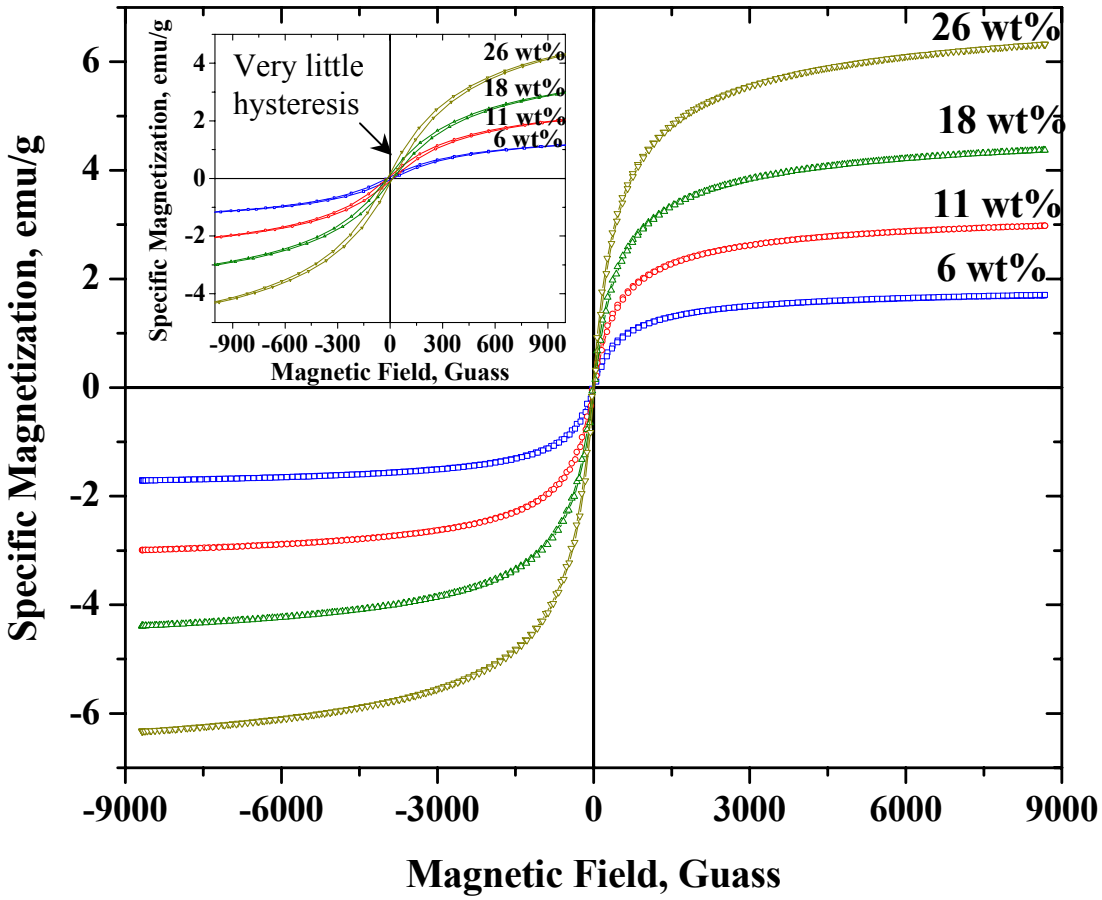

Figure 4.6 Specific magnetic saturation vs. magnetic field of electrospun Estane®-MnZnFe-Ni composite fibers at different wt% of MnZnFe-Ni nanoparticles. The inset shows the specific magnetization at/and near zero magnetic field region.

wt% loading of the nanoparticles on Estane® fibers (Figure 4.7b). Again, a linear correlation with a high regression coefficient was observed (R^2=0.999).

These investigations indicate that flexible superparamagnetic substrates were successfully processed via electrospinning. Further tests are currently underway to determine the magnetic response of these substrates at high frequencies.

4.5 Conclusions

Flexible field responsive superparamagnetic substrates were prepared by electrospinning a solution of Estane®, a segmented polyester based segmented polyurethane, containing ferrite nanoparticles (ca. 14 nm) of mixed Mn-Zn-Ni. The flexible mats were characterized in terms of fiber morphology and magnetic properties.

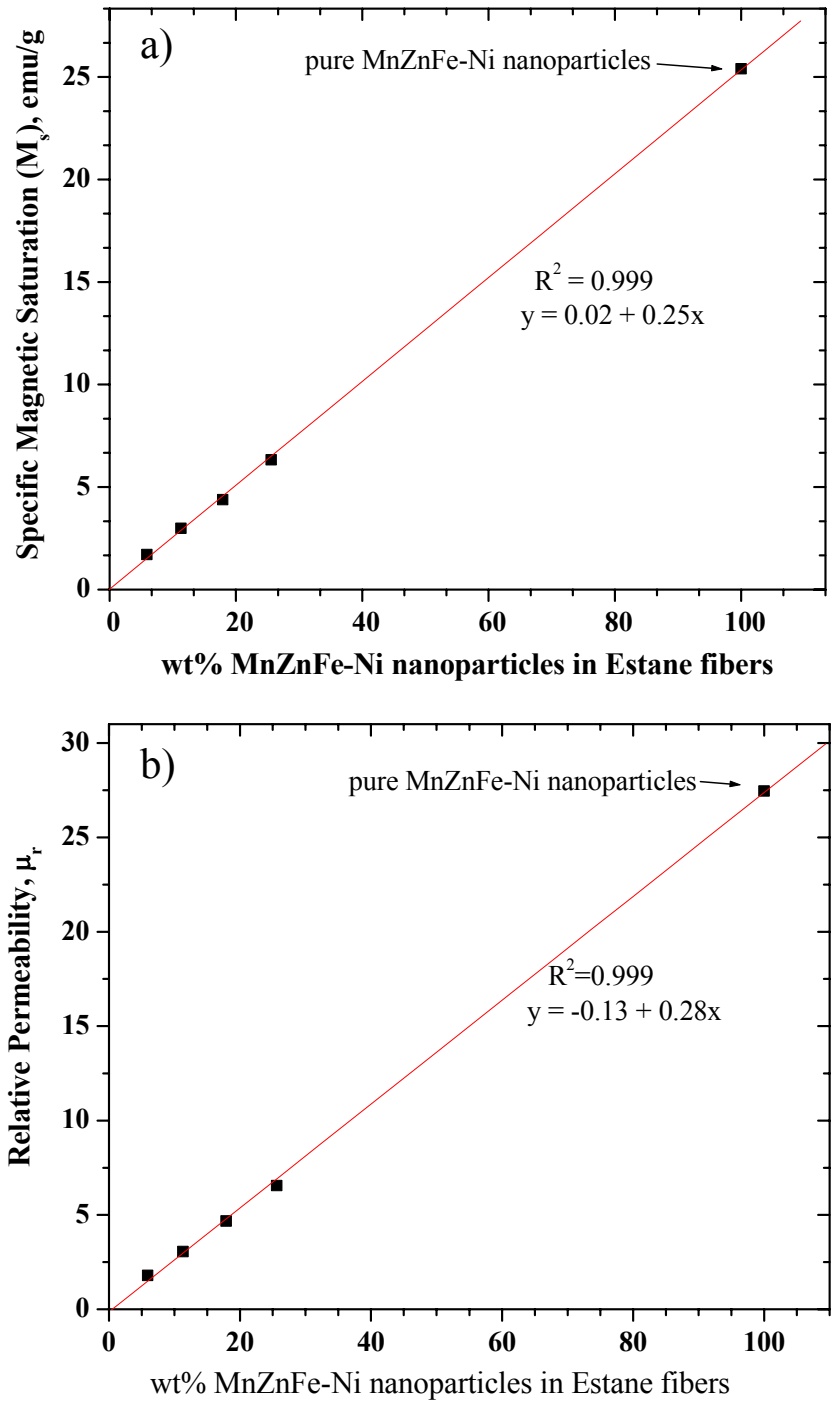

Figure 4.7 Magnetic saturation (M_S) and b) relative permeability of electrospun Estane®-MnZnFe-Ni composite submicron fibers as a function of wt% of MnZnFe-Ni nanoparticles.

FESEM of the electrospun substrates indicated that the diameter of these composite fibers was ca. 300-500 nm. Furthermore, the back-scattered electron FESEM images indicated agglomeration of the nanoparticles at higher wt% (ca 17-26 wt%) loading on the electrospun fibers. The induced specific magnetic saturation and the relative permeability were found to increase with increasing wt% loading of the ferrite nanoparticles on the submicron electrospun fibers. A specific magnetic saturation of 1.7 – 6.3 emu/g at ambient conditions indicated superparamagnetic behavior of these composite electrospun substrates.

Acknowledgements

This material is based upon work supported by, or in part by, the U.S. Army Research Laboratory and the U.S. Army Research Office under grant number DAAD19-02-1-0275 Macromolecular Architecture for Performance (MAP) MURI. The author thanks Prof. R. O. Claus and Ramazan Asmatulu for their collaboration. The author would also like to thank Prof. Chip Frazier, Wood Science Department, Virginia Tech, for allowing the use of AR-1000 Rheometer for viscosity measurements.

References

(1) Thurn-Albrecht, T.; Schotter, J.; Kastle, G. A.; Emley, N.; Shibauchi, T.; Krusin-Elbaum, L.; Guarini, K.; Black, C. T.; Tuominen, M. T.; Russell, T. P. *Science (Washington, D. C.)* **2000**, *290*, 2126-2129.

(2) Allwood, D. A.; Xiong, G.; Cooke, M. D.; Faulkner, C. C.; Atkinson, D.; Vernier, N.; Cowburn, R. P. *Science (Washington, DC, United States)* **2002**, *296*, 2003-2006.

(3) Allwood, D. A.; Vernier, N.; Xiong, G.; Cooke, M. D.; Atkinson, D.; Faulkner, C. C.; Cowburn, R. P. *Applied Physics Letters* **2002**, *81*, 4005-4007.

(4) Markov, E. M.; Pinchuk, L. S.; Goldade, V. A.; Gromyko, Y. V.; Choi, U. S. *Trenie i Iznos* **1995**, *16*, 518-522.

(5) Epstein, A. J.; Miller, J. S. *Synthetic Metals* **1996**, *80*, 231-237.

(6) Jones, W. E., Jr.; Dong, H.; Nyame, V.; Ochanda, F. *Annual Technical Conference - Society of Plastics Engineers* **2003**, *61st*, 1948-1950.

(7) Jones, W. E., Jr. *Abstracts of Papers, 226th ACS National Meeting, New York, NY, United States, September 7-11, 2003* **2003**, POLY-566.

(8) Dikeakos, M.; Tung, L. D.; Veres, T.; Stancu, A.; Spinu, L.; Normandin, F. *Materials Research Society Symposium Proceedings* **2002**, *734*, 315-320.

(9) Fert, A.; Piraux, L. *Journal of Magnetism and Magnetic Materials* **1999**, *200*, 338-358.

(10) Snelling, E. C. *Soft Ferrites: Properties and Applications*, 1969.

(11) Snelling, E. C. *Proc. Brit. Ceram. Soc.* **1964**, *2*, 151-174.

(12) Snelling, E. C. *IEEE Spectrum* **1972**, *9*, 42-51.

(13) Thakur, A.; Singh, M. *Ceramics International* **2003**, *29*, 505-511.

(14) Morrison, S. A.; Cahill, C. L.; Carpenter, E. E.; Calvin, S.; Harris, V. G. *Journal of Applied Physics* **2003**, *93*, 7489-7491.

(15) Wang, J.; Zeng, C.; Peng, Z.; Chen, Q. *Physica B: Condensed Matter (Amsterdam, Netherlands)* **2004**, *349*, 124-128.

(16) Wang, M.; Singh, H.; Hatton, T. A.; Rutledge, G. C. *Polymer* **2004**, *45*, 5505-5514.

(17) Doshi, J.; Reneker, D. H. *Journal of Electrostatics* **1995**, *35*, 151-160.

(18) Fong, H.; Chun, I.; Reneker, D. H. *Polymer* **1999**, *40*, 4585-4592.

(19) Kim, J.-S.; Reneker, D. H. *Polymer Engineering and Science* **1999**, *39*, 849-854.

(20) Deitzel, J. M.; Kleinmeyer, J. D.; Hirvonen, J. K.; Beck Tan, N. C. *Polymer* **2001**, *42*, 8163-8170.

(21) Srinivasan, G.; Reneker, D. H. *Polymer International* **1995**, *36*, 195-201.

(22) Koombhongse, S., 2001; p 172 pp.

(23) Koombhongse, S.; Liu, W.; Reneker, D. H. *Journal of Polymer Science, Part B: Polymer Physics* **2001**, *39*, 2598-2606.

(24) Schreuder-Gibson, H. *International Conference on Textile Coating & Laminating: Preparing for the Future--A New Millenium, 8th, Frankfurt, Germany, Nov. 9-10, 1998* **1998**, Paper No17/11-Paper No17/24.

(25) Matthews, J. A.; Wnek, G. E.; Simpson, D. G.; Bowlin, G. L. *Biomacromolecules* **2002**, *3*, 232-238.

(26) Matthews, J. A.; Boland, E. D.; Wnek, G. E.; Simpson, D. G.; Bowlin, G. L. *Journal of Bioactive and Compatible Polymers* **2003**, *18*, 125-134.

(27) Reneker, D. H.; Yarin, A. L.; Fong, H.; Koombhongse, S. *Journal of Applied Physics* **2000**, *87*, 4531-4547.

(28) Yarin, A. L.; Koombhongse, S.; Reneker, D. H. *Journal of Applied Physics* **2001**, *90*, 4836-4846.

(29) Yarin, A. L.; Koombhongse, S.; Reneker, D. H. *Journal of Applied Physics* **2001**, *89*, 3018-3026.

(30) Hohman, M. M.; Shin, M.; Rutledge, G.; Brenner, M. P. *Physics of Fluids* **2001**, *13*, 2221-2236.

(31) Hohman, M. M.; Shin, M.; Rutledge, G.; Brenner, M. P. *Physics of Fluids* **2001**, *13*, 2201-2220.

(32) Wang, X.; Lee, S.-H.; Drew, C.; Senecal, K. J.; Kumar, J.; Samuelson, L. *Abstracts of Papers, 222nd ACS National Meeting, Chicago, IL, United States, August 26-30, 2001* **2001**, PMSE-366.

(33) Lee, S.-H.; Ku, B.-C.; Wang, X.; Samuelson, L. A.; Kumar, J. *Materials Research Society Symposium Proceedings* **2002**, *708*, 403-408.

(34) Zhang, Y.; Dong, H.; Norris, I. D.; MacDiarmid, A. G.; Jones, W. E., Jr. *Abstracts of Papers, 222nd ACS National Meeting, Chicago, IL, United States, August 26-30, 2001* **2001**, PMSE-369.

(35) Fong, H.; Liu, W.; Wang, C.-S.; Vaia, R. A. *Polymer* **2001**, *43*, 775-780.

(36) Deitzel, J. M.; Kosik, W.; McKnight, S. H.; Tan, N. C. B.; DeSimone, J. M.; Crette, S. *Polymer* **2002**, *43*, 1025-1029.

(37) Boland, E. D.; Bowlin, G. L.; Simpson, D. G.; Wnek, G. E. *Abstracts of Papers, 222nd ACS National Meeting, Chicago, IL, United States, August 26-30, 2001* **2001**, PMSE-031.

(38) Boland, E. D.; Matthews, J. A.; Pawlowski, K. J.; Simpson, D. G.; Wnek, G. E.; Bowlin, G. L. *Frontiers in Bioscience* **2004**, *9*, 1422-1432.

(39) Boland, E. D.; Simpson, D. G.; Wnek, G. E.; Bowlin, G. L. *Polymer Preprints (American Chemical Society, Division of Polymer Chemistry)* **2003**, *44*, 92-93.

(40) Boland, E. D.; Simpson, D. G.; Wnek, G. E.; Bowlin, G. L. *Abstracts of Papers, 226th ACS National Meeting, New York, NY, United States, September 7-11, 2003* **2003**, POLY-533.

(41) Boland, E. D.; Wnek, G. E.; Simpson, D. G.; Pawlowski, K. J.; Bowlin, G. L. *Journal of Macromolecular Science, Pure and Applied Chemistry* **2001**, *A38*, 1231-1243.

(42) Boland Eugene, D.; Matthews Jamil, A.; Pawlowski Kristin, J.; Simpson David, G.; Wnek Gary, E.; Bowlin Gary, L. *Frontiers in bioscience : a journal and virtual library* **2004**, *9*, 1422-1432.

(43) Kenawy, E.-R.; Bowlin, G. L.; Mansfield, K.; Layman, J.; Sanders, E.; Simpson, D. G.; Wnek, G. E. *Polymer Preprints (American Chemical Society, Division of Polymer Chemistry)* **2002**, *43*, 457-458.

(44) Kenawy, E.-R.; Abdel-Fattah, Y. R. *Macromolecular Bioscience* **2002**, *2*, 261-266.

(45) Gibson, P.; Schreuder-Gibson, H.; Pentheny, C. *Journal of Coated Fabrics* **1998**, *28*, 63-72.

(46) Orlicki, J. In *ACS POLY Workshop on Branched Polymers*; ACS: Williamsburg, VA, 2004.

(47) Pifarre-Montaner, E.; Caldwell, G.; Dasgupta, S.; Goddard III, W. A. Materials and Process Simulation Center (139-74), Beckman Institute, California Institute of Technology, Pasadena, CA 91125, USA, Modeling Thermoplastic Polyurethanes: Estane, *from* http://www.wag.caltech.edu/msc99/talks/e5/

(48) Tkatch, V. I.; Rassolov, S. G.; Popov, V. V.; Kameneva, V. Y.; Petrenko, O. A. *Materials Letters* **2004**, *58*, 2988-2992.